

Performance evaluation of drying shrinkage and durability in pavement quality concrete with recycled aggregate, ggbs and I-crete

Chittibabu B.^{1*} and Rani K.D.²

¹Research Scholar, Civil Engineering Department, Andhra university, Visakhapatnam, Andhra Pradesh, India.

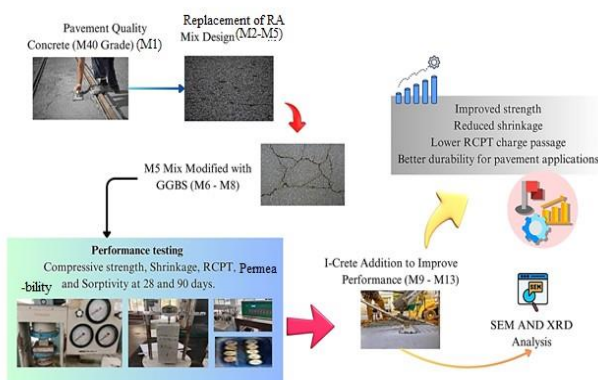
²Professor, Civil Engineering Department, Andhra university, Visakhapatnam, Andhra Pradesh, India.

Received: 28/09/2024, Accepted: 16/11/2024, Available online: 19/11/2024

*to whom all correspondence should be addressed: e-mail: bchittibabu.rs@andhrauniversity.edu.in

<https://doi.org/10.30955/gnj.006845>

Graphical abstract



Abstract

The study examines replacement of Natural Aggregates (NA) with Recycled Aggregate (RA) in Pavement Quality Concrete (PQC) M40 grade (M1) with 25%, 50%, 75% and 100% RA replacing NA in M2, M3, M4 and M5 mixes. The compressive strength decreases with higher RA, but all mixes reach the target strength at 28 and 90 days. M5 was tested by adding Ground Granulated Blast furnace Slag (GGBS) in increments of 5% to 15% in M6, M7 and M8 to reduce the cement content. The main performance parameters include compressive strength, drying shrinkage, water penetration, Rapid Chloride Permeability Test (RCPT) at 28 and 90 days and sorptivity at 28 days. M5 reduced compressive strength but increased drying shrinkage, sorptivity, penetration depth and RCPT charge passage. Increasing the GGBS by 10% in M7 improved the strength, while increasing the GGBS by 15% in M8 decreased the strength compared to M1 and M5. To address strength degradation, the study incorporated 2% I-Crete along with GGBS in 5% increments from 15% to 35% in M9 to M13 mixes. M11 mix (2% I-Crete, 25% GGBS) showed better strength, reduced shrinkage and lower RCPT charge, ensuring better durability for SEM and XRD pavement applications.

Keywords: RA, Drying shrinkage, GGBS, I-Crete, RCPT, sorptivity, penetration depth

1. Introduction

The swift growth of global economies and construction activities has raised concern about the degradation of natural resources and management of concrete waste. The construction sector, a major contributor to environmental deterioration, consumes a significant amount of natural resources and generates around 10 billion tons of construction debris worldwide each year, around thirty percent of the entire amount of solid waste (Mao *et al.* 2021; Singh & Singh 2021). The increasing environmental impact underscores the need for sustainable practices, such as incorporating RA into concrete mixtures. By reducing total natural demand, RA has major positive impacts on the environment, economy and society (Silva *et al.* 2019; Tam *et al.* 2018).

This research continues to explore the optimal use of RA in highway pavement concrete, emphasizing its role in developing sustainable construction practices.

GGBS, a by-product of the iron and steel producing process, has been widely used as a Supplementary Cementitious Material (SCM) in concrete construction due to its environmental benefits and its ability to improve concrete durability (Lim.y *et al.* 2021). Studies have demonstrated that partially replacing Portland cement with GGBS effectively reduces the carbon footprint of the construction industry while supporting sustainable practices (Hwang J *et al.* 2013). The incorporation of GGBS, along with other SCMs. This includes fly ash and silica fume, to significantly improve both the mechanical properties and durability of concrete. Replacing 30% of cement with GGBS and 50% with coal fly ash has resulted in marked improvements in concrete performance (Wang *et al.* 2021). The mechanical properties of the concrete mixture are lower at the early stage (7 days) but reach maximum strength at a later stage (90 days) due to the lower strength heat of hydration. The finer GGBS particles enhance the concrete's microstructure and pore

distribution, leading to reduced shrinkage, increased durability, and improved stability by making the concrete denser (Zhang *et al.* 2023; Hwang *et al.* 2013).

I-Crete, a high-quality mineral additive compliant with ASTM C1797 and IS 2645, is highly reactive and has a well-regulated particle size, with less than 10% retained on a 45-micron sieve.

The present phase of research focuses on optimizing the use of GGBS in highway pavement concrete, with an emphasis on its role in advancing sustainable construction practices. This study analyzes the impact of GGBS on the mechanical properties and durability of concrete, particularly in the context of highway pavements. It investigates the optimal replacement levels of GGBS to achieve maximum strength and durability, while also assessing the effects on shrinkage and stability due to alterations in concrete's microstructure and pore distribution. The goal is to identify the most effective use of GGBS to improve the performance and sustainability of highway concrete pavement.

The study investigates the optimal use of RA in PQC. It examines the effects of substituting NA with RA and further replacing cement with GGBS, in addition to incorporating I-Crete. The study aims to determine whether these substitutions help achieve the target strength and enhance concrete performance. By varying percentages of RA, GGBS, and I-Crete, the research evaluates their impact on concrete strength and durability at both early and later stages. This approach seeks to provide a sustainable solution for concrete pavements, improving long-term durability and environmental benefits while addressing the increasing demand for recycled materials in the industry.

1.1. Research significance

The study advances sustainable PQC by exploring the maximum replacement of NA with RA. It addresses a key gap in understanding RA application in pavement construction. By utilizing GGBS as a partial cement replacement and incorporating I-Crete.

The study aims to improve the compressive strength and durability of PQC in this paper, the key parameters examined include compressive strength, drying shrinkage, durability, chloride ion diffusion resistance, sorptivity, and water penetration. Parameter of findings provides insights into reducing the carbon footprint of PQC, promoting environmental sustainability, and supporting the use of recycled materials in pavement construction.

2. Materials and mix proportions

2.1. Data collection

In this research, RA with a nominal size of 20-10 mm was sourced from Construction and demolition waste plant, facility in Hyderabad, Telangana. River sand conforming to Zone-II as per IS 383-2016 and OPC 53 grade cement from Visakhapatnam were used. In the mix Additionally, GGBS and I-Crete were procured from Visakhapatnam and Chennai, respectively. Potable water and CONPLAST SP 430 chemical admixture were used as per IS 456-2000.

Based on the trial studies performed with different dosages of I-crete, the outcomes indicated that the optimum results are observed with 2% of I-Crete. Based on the test outcomes of trial studies, 2% I-crete was chosen as optimum percentage.

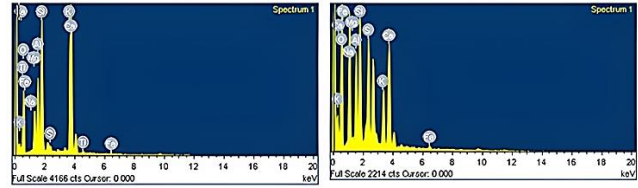


Figure 1 (a) GGBS spectrum (b) I-Crete Spectrum

2.2. Data measurement

The study adhered to standard testing protocols for durability parameters, including sorptivity, RCPT, and water penetration. Sorptivity was measured as per ASTM C1585, which quantifies the absorption of water by concrete over time. RCPT was conducted following ASTM C1202, which measures the charge passed through concrete as a proxy for chloride ion permeability. For water penetration depth, the study followed IS 516: Part 2: Sec 1, ensuring consistency and accuracy in the evaluation of the concrete's resistance to water ingress, critical for assessing durability in pavement applications.

2.3. Physical characterization

Physical characteristics of the materials were as follows: NA had a specific gravity of 2.84, bulk density (Compacted) of 1800 kg/m³, aggregate impact value of 18.96%, and aggregate crushing value of 18.01%. In contrast, RA exhibited a lower specific gravity of 2.60, bulk density (Compacted) of 1600 kg/m³, and higher impact and crushing values of 23.40% and 25.47%, respectively. Cement had a specific gravity of 3.15 and a standard consistency of 30%, GGBS had a specific gravity of 2.90 and a consistency of 32%, as shown in the EDAX spectrum in Figure (a). I-Crete had a specific gravity of 2.43 and a consistency of 22%, as illustrated by the EDAX spectrum in Figure 1(b). RA having lower Physical and mechanical characteristics as compared to NA, RA complies with IS 383-2016 and MORTH standards and was used under Saturated Surface Dry (SSD) conditions. The inclusion of I-Crete as an additive in the study plays a crucial role in enhancing the durability of PQC, particularly when replacing higher proportions of natural aggregates with RA. Unlike traditional additives, I-Crete has been shown to reduce the detrimental effects of RA on compressive strength and drying shrinkage. By incorporating I-Crete, especially in mixes with higher RA content, the study found improvements in strength retention and reduction in shrinkage, which are essential for enhancing the long-term durability of concrete structures, particularly in pavement applications.

2.4. Mix proportions

The mix design for M40 grade concrete followed IRC-44-2017, IRC-15-2017, and IS 10262-2019 standards. RA was used in a 60:40 ratio, with 60% of the coarse aggregate (20-10 mm) replaced by natural aggregate at 25% intervals, and the remaining 40% consisting of 10 mm

natural aggregate. GGBS was used at 5% intervals, replacing 5-35% of OPC, and 2% I-Crete was added to

improve bonding in PQC. All mix notations as shown in **Table 1**.

Table 1. Mix notations

Mix Id's	Mix notations
MNAC	M1
MRCA-25	M2
MRCA-50	M3
MRCA-75	M4
MRCA-100	M5
MRCA-100+5%GGBS	M6
MRCA-100+10%GGBS	M7
MRCA-100+15%GGBS	M8
MRCA-100+15%GGBS+2I	M9
MRCA-100+20%GGBS+2I	M10
MRCA-100+25%GGBS+2I	M11
MRCA-100+30%GGBS+2I	M12
MRCA-100+35%GGBS+2I	M13

Note: MNAC: Mix Notation of Natural aggregate Concrete, MRCA: Mix of Recycled Concrete Aggregate, GGBS: Ground Granulated Blast Furnace Slag, RA=Recycled Aggregate, SCM=Supplementary Cementitious Material, I=I-crete (2%)

2.5. Studies on hardened concrete

Concrete compressive strength was measured using standard 100 x 100 x 100 mm cubes in accordance with IS 516: Part 1: Section 1: 2021. **Figure 2** shows the experimental setup. Drying shrinkage is tested by IS 516 (Part 6): 2020, micrometer gauge or dial gauge to 0.001 mm. Samples were prepared with mould dimensions of 75 x 75 x 300 mm and a vibrating table operating at minimum 40 Hz (as per IS 2514) was used for filling.



Figure 3. Test setup for Drying Shrinkage

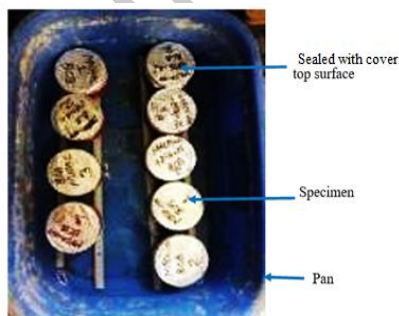


Figure 4. Test setup for Sorptivity

At least three samples were evaluated and the shrinkage was estimated as a percentage of strain. **Figure 3** illustrates the experimental setup.

Sorptivity was tested using disc specimen of 100±6 mm diameter and 50±3 mm depth, according to ASTM C1585-04. After oven-drying, the samples were partially submerged in water and their mass was measured regularly for 7 days to measure water absorption. **Figure 4** shows the experimental setup. RCPT (ASTM C1202-12) used cylindrical specimens with 100 mm diameter and 50±3 mm depth aged 28 and 90 days (according to C192/C192M).

The samples were sealed with low- or high-viscosity sealants and the electrical conductivity was measured at 60 V over a period of 6 hours. **Figure 5** shows the experimental setup. Water penetration depth was tested as per IS 516 (Part 2/Sec 1): 2018 using cylindrical specimen with 100 mm diameter and 100 mm depth.

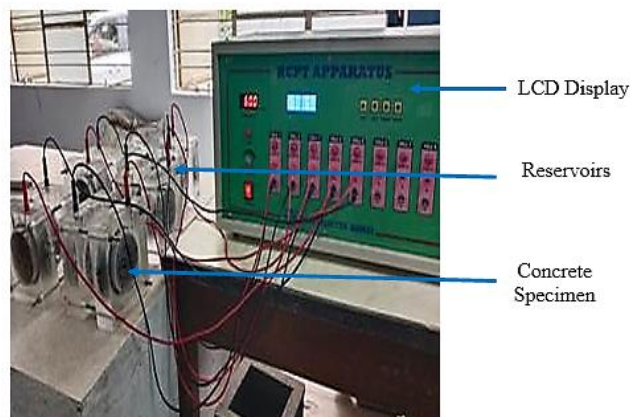


Figure 5. Test setup for Rapid Chloride Permeability Test

The sample was held under a water pressure of 500±50 kPa for 72±2 hours, the sample was split with the experimental setup shown in Figure 6. and the penetration depth was measured.



Figure 6. Test setup for Depth of penetration of water

3. Results and discussion

3.1. Compressive strength

The compressive strength of concrete diminishes as natural aggregates (NA) are progressively replaced by recycled aggregates (RA) in 25% increments, up to 100%, as observed in the control mix (M1) through M5. Specifically, compressive strength at 28 days decreased from 51.20 MPa to 48.30 MPa, and at 90 days from 52.81 MPa to 49.80 MPa, largely due to the weaker interfacial transition zone (ITZ), higher porosity, and reduced mechanical properties of RA compared to NA (Jindal & Ransinchung, 2018; Wang *et al.* 2021; IRC:121-2017; Kou *et al.* 2011). However, all RA-replaced mixes still met the strength criteria set by IRC 58:2017 and IRC-44:2017. The study further analyzed the impact of ground granulated blast-furnace slag (GGBS) on mixes with 100% RA, where GGBS replacement of cement in 5–35% increments resulted in a maximum compressive strength reduction of 4.68% at 28 days and 4.75% at 90 days in the M7 mix. Improved strength in M7 over M5 is attributed to GGBS's fine particles and enhanced C-S-H gel formation (Hwang *et al.* 2013; Kou *et al.* 2011; Sharma *et al.* 2021). In mixes with higher GGBS content, such as M6, reduced early-age strength and delayed pozzolanic reactions led to a decline in compressive strength (Kumar *et al.* 2023; Sharma *et al.* 2021). Notably, mix M11, with 25% GGBS and 2% I-Crete, demonstrated improved compressive strengths of 51.30 MPa and 52.91 MPa at 28 and 90 days, respectively, I-Crete's role in promoting hydration and enhancing the concrete's microstructure. For visual reference, these results are depicted in Figure 7.

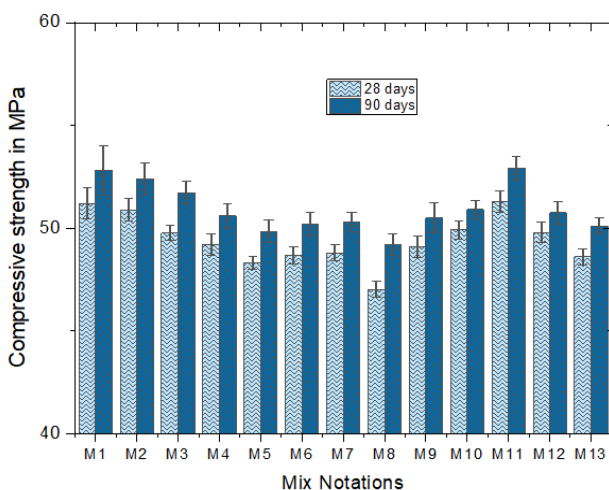


Figure 7. Variation of compressive strength Vs Mix notations for 28 and 90 days curing period

The selection of specific Recycled Aggregate (RA) replacement percentages, ranging from 25% to 100%, was based on evaluating the trade-offs between maintaining the compressive strength of Pavement Quality Concrete (PQC) while utilizing RA for sustainable construction. The impact of RA on compressive strength was observed to decrease as RA content increased. However, all mixes achieved the target strength at 28 and 90 days, demonstrating the feasibility of higher RA usage. The choice of these percentages allows a balanced approach to optimizing the use of RA without compromising on performance, while offering a solution to reduce reliance on natural aggregates.

To support the compressive strength results, statistical analysis such as standard deviation and coefficient of variation can provide insights into the variability of strength across different mixes. For example, while the compressive strength decreases with higher RA content (M5), the statistical data confirms that all mixes, including those with 100% RA, reach the target strength at 28 and 90 days. The analysis demonstrates the consistency of the results and supports the feasibility of using RA up to 100% in PQC without compromising structural integrity.

3.2. Drying shrinkage

The substitute of NA with RA in the control mix (M1) led to increased drying shrinkage. Specifically, when compared to M1 mix, M5 mix showed approximately 4.92 times higher strain levels after 28 days and 3.71 times higher strain levels at 90 days. This substantial increase in strain for the M5 mix is attributed to the utilize of RA, as Drying shrinkage increases with the replacement of RA due to its higher porosity and weaker ITZ, which lead to greater moisture loss and internal voids. (Duan and Poon 2014; Mao *et al.* 2021; Yu Y *et al.* 2021).

For M7 mix, strain values were approximately 3.64 and 2.60 times higher than M1 mix at 28 and 90 days, accordingly. Although the M7 mix showed increased drying shrinkage compared to the M1 mix, it was lower than that of the M5 mix. Adding GGBS to the mix decreases drying shrinkage by improving the pore structure and reducing porosity through its pozzolanic reaction, which leads to a denser matrix (Kumar and Mishra 2022; Zhag.W *et al.* 2015; Mao *et al.* 2021). M11 mixture exhibited 1.89 times greater strain value at 28 days and 1.31 times greater at 90 days than M1 mixture. The M11 mix showed the least increase in strain compared to the M1 mix, indicating more stable performance over time. As RA content increases, the shrinkage also increases, as observed in M5. The higher absorption capacity of RA leads to more significant volume changes during drying, which results in increased drying shrinkage. This behavior examines the need for additives like GGBS and I-Crete to mitigate the adverse effects of RA on shrinkage and enhance the long-term stability of the concrete. This result highlights the effect of adding I-Crete, It reduces porosity and improves the microstructure of concrete, and strengthens the ITZ, thereby reducing drying shrinkage strain. The results are shown in Figure 8. GGBS and I-Crete work synergistically

to counteract the reduction in compressive strength with higher RA content by improving the microstructure and reducing the effects of porosity. GGBS, as a SCM, enhances the hydration process, improving the strength and durability of the concrete, while I-Crete enhances the bonding between particles and reduces shrinkage. In the M9 to M13 mixes, the combination of 2% I-Crete and GGBS in varying proportions effectively mitigated the strength loss observed with high RA content, particularly in M11 (2% I-Crete, 25% GGBS), which showed improved strength and reduced shrinkage

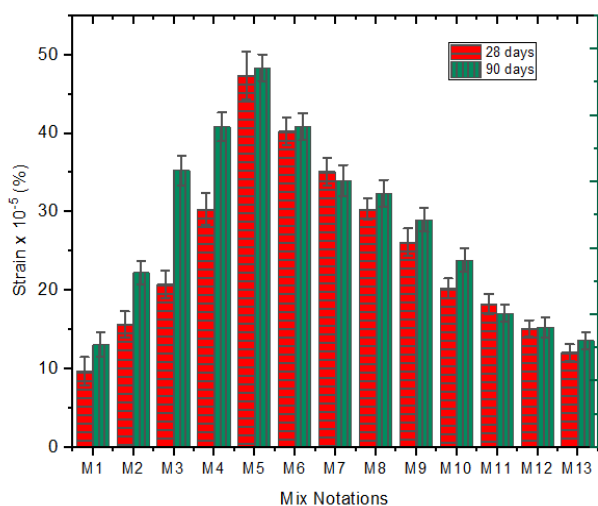


Figure 8. Variation of Drying shrinkage (Strain in %) Vs Mix notations for 28 and 90 days curing period

The drying shrinkage behavior of each mix was compared to similar studies in the field of pavement concrete with RA. Studies have shown that higher RA content typically results in increased shrinkage due to the higher water absorption and porous nature of RA. The drying shrinkage observed in the M5 mix (100% RA) aligns with these findings, demonstrating that although higher RA content may improve sustainability, it introduces challenges in shrinkage, which must be mitigated with appropriate additives like GGBS and I-Crete to achieve better performance.

3.3. The rapid chloride permeability test (RCPT)

Rapid Chloride Permeability Test (RCPT) and Water penetration values were measured using standard testing procedures outlined by ASTM: C1202. and IS:516:part2:sec1codes. The water penetration depth was evaluated by placing the concrete samples under a consistent water pressure for a specified period, The depth of water penetration into the concrete specimens under pressure was measured. The RCPT was performed by applying a constant 60V voltage across 100 mm diameter and 50 mm thick concrete specimens to measure the charge passed, which indicates permeability and chloride ion penetration resistance. Initial absorption was measured every half hour for up to six hours, and secondary absorption was measured every 24 hours for up to eight days. These tests were performed on all mixes at 28 and 90 days to evaluate the durability and potential for corrosion in different mixes.

As RA was incorporated in the M1 mix, the overall charge passed increased. However, all mixes M1 through M13 had charge passage levels within acceptable limits per ASTM C1202-12 for 28 and 90 days of curing. In mix M5, RCPT charge passes increased by 97.37% and 89.21% examined to M1 mix at 28 and 90 days, respectively. RA increases porosity because of the mortar debris on its surface, resulting in higher RCPT charge passage. This in turn, creates voids in the concrete and weakens its resistance to chloride diffusion when subjected to an electrical charge (Jun Phil Hwang *et al.* 2013; Wang.B *et al.* 2021).

For M7 mix, charge passage increased by 60.95% and 59.89% at 28 and 90 days compared to M1. However, compared to M5, the charge resistance improved for both curing periods due to as the GGBS percentage increases, It forms extra C-S-H gel when it combines with calcium hydroxide, which fills voids and reduces the porosity of the concrete. This denser microstructure hinders the movement of chloride ions (Kyong and Kyum 2005).

Further tests on M9 to M13 mixes with 2% I-Crete and incremental GGBS additions revealed that the RCPT charge passage for the M11 mix was reduced by 0.37% and 1.35% at 28 and 90 days, respectively, compared to M1. This reduction due to the I-Crete heterogeneous mixture of calcium, silicon, and aluminum oxides, which create a dense pore structure through secondary hydration reactions beyond just C-S-H gel formation. Additionally, prolonging the curing age significantly reduced charge passage from 28 to 90 days in RA with GGBS composites, as it results in a denser bond at later stages (Jain.J *et al.* 2012.; Lim *et al.* 2021), a trend shown in Figure 9.

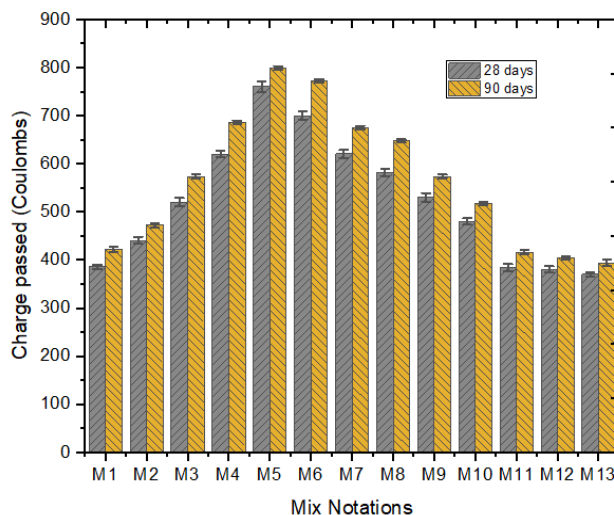


Figure 9. Variation of Charge passed Vs Mix notations for 28 and 90 days curing period

3.4. Sorptivity

The Replacement of RA in the control mix M1 leads to an increase in sorptivity. The sorptivity was higher in M5 mix in both primary and secondary observations at 28 days of curing as comparison to M1 mix. RA content, adherent mortar and weak ITZ structure, contribute to this increase. Similar trends have been observed by other researchers,

indicating that as RA increases, sorptivity also increases (Kanellopoulos *et al.* 2014; Olorunsogo and Padayachee, *et al.* 2002).

When GGBS was added up to 10% in the M7 mix, the sorptivity coefficient decreased. The M7 mix achieved optimum strength with GGBS because the ultra-fine particles of GGBS filled the voids, densified the microstructure, increased homogeneity, and promoted C-S-H gel formation. The improved binding and refined pore structure resulted in reduced sorptivity, although it remained higher at 28 days than in the M1 mix (Rama Krishna *et al.* 2021; Majhi and Naik 2019; Jindal and Ranginchang 2017).

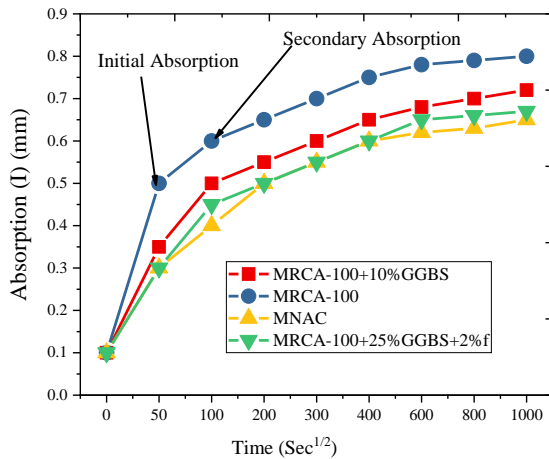


Figure 10. Variation of Absorption with Vs Time ($\sqrt{\text{Sec}}$) for all four mixes at 28 days curing period

Addition of I-Crete from M9 to M13 revealed that M11 mix exhibited significant reduction in sorptivity with a lower value than M1 mix. I-Crete acts as a highly reactive blended material, forming a dense structure by filling voids and undergoing secondary reactions beyond the formation of a C-S-H gel. The reduction in sorptivity coefficient in the M11 mix highlights the beneficial impact of mineral admixtures on performance of concrete pavements. As curing periods increase, Sorptivity decreases with extended curing as a denser structure forms, and GGBS's low heat of hydration aids bond formation in later stages and For all four optimum mixes, durability and sorptivity classes are rated as good to excellent, measured in absorbance $\text{mm/hr}^{0.5}$ according to source classification (Krishna *et al.* 2021), as the result are shown in **Figure 10**.

3.5. Water depth penetration of water under pressure

The depth of water penetration increases with the percentage of incorporated RA up to M5 mix, where the value of penetration at 28 days for M5 mix is 30 mm. According to DIN 1048 and source data from (Krishna *et al.* 2021) this represents an intermediate classification. For the M5 mix, examined to the M1 mix, the penetration depth increases by 2.72 and 2.69 times at 28 and 90 days of curing, respectively. However, the total water permeability values were low for all the mixes except M5 mix. This increase in penetration can be attached to the

pore structure, weak ITZ and mortar adhering to the aggregate (Thomas *et al.* 2013; Zega *et al.* 2014).

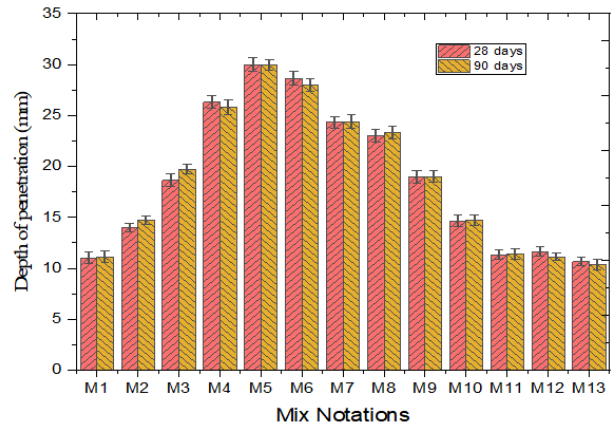


Figure 11. Variation of Depth of penetration with different curing periods for different mixes

In M7 mix containing optimum ratio of GGBS and RA, compared to M1, the penetration depth was 2.21 and 2.19 times higher at 28 and 90 days, respectively. However, it shows better penetration depth compared to M5. This decrease is due to the fine particles of GGBS, which generate less heat during hydration and contribute to the creation of C-S-H gel, filling the microstructure (Majhi and Naik 2019). The addition 2% of I-Crete in mixes M9 to M13, especially mix M11, This led to a noticeable decrease in penetration depth by 1.03 and 1.02 times at 28 and 90 days of curing, respectively, examined to M1. The M11 mix performed better than the control mix. I-Crete improves the bonding structure and helps to form extra bonds than C-S-H gel, making the structure denser. As the concrete ages and undergoes curing, the penetration depth decreases (Thomas *et al.* 2013; Zega *et al.* 2014). This trend is illustrated in **Figure 11**.

4. Morphological analysis

4.1. Scanning electron microscopic (SEM) analysis

SEM is a popular technique for examining the microstructure of solids, providing high-resolution images that reveal object shapes and variations in chemical composition, as per the guidelines of Designation: C1723 - 10. SEM was used to study the fracture surfaces of RA with different mineral contents, focusing on samples cured for 28 days. **Figure 12 (a)** illustrates the microstructure of M1. mix at the virgin aggregate-cement interface, highlighting the presence of C-S-H gel and hydroxide compounds. In contrast, **Figure 12 (b)** depicts the M5 mix, which differs from ordinary concrete due to the mortar adhering from the old cement matrix, leading to the creation of two distinct ITZs. The M5 mix shows abundant needle-like and hexagonal ettringite, as well as more Portlandite calcium hydroxide particles. This mix also exhibits excess calcium hydroxide with incomplete hydration, voids, and a weak ITZ. This weak ITZ, due to the loosely bonded mortar, disrupts the aggregate bond, reducing overall strength (Bonifazi *et al.* 2015; Ahmad *et al.* 2022).

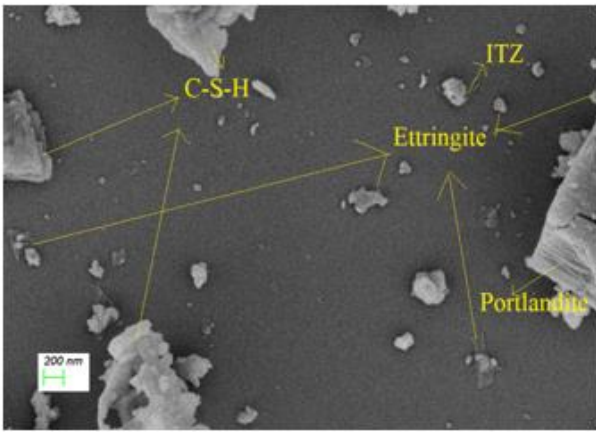


Figure 12 (a) MNAC (M1) Mix

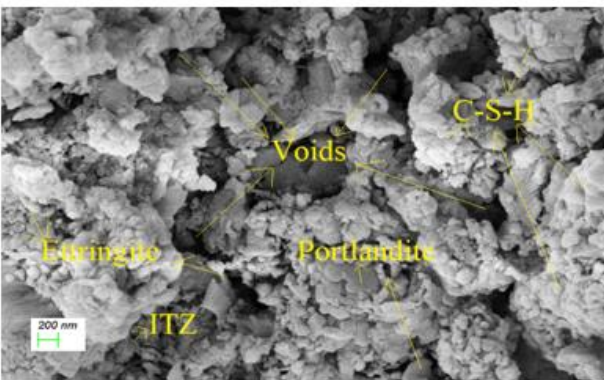


Figure 12 (b) MRCA-100(M5) Mix

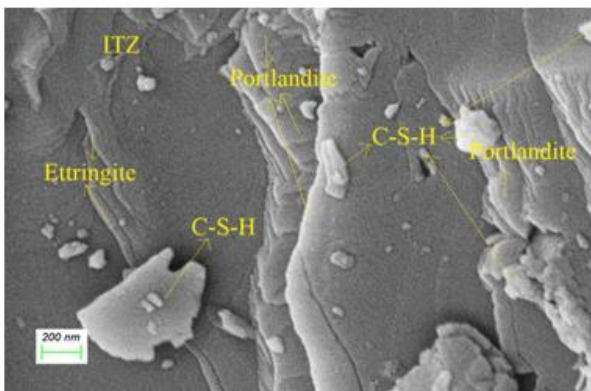


Figure 12 (c) MRCA-100+10%GGBS (M7) Mix

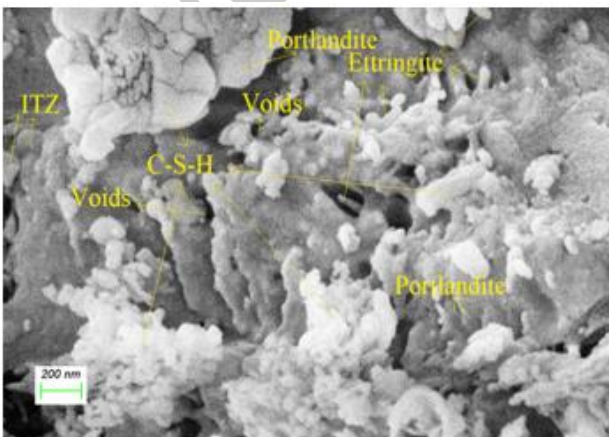


Figure 12 (d) MRCA-100+25%GGBS+2I (M11) Mix

Figure 12(c) shows the M7 mix, revealing finer GGBS particles, which improve the creation of C-S-H gel, fill the

gaps in voids and ITZ, enhance packing efficiency, reduce voids, and distribute stress more evenly. The smooth surfaces and improved workability of these particles contribute to strong ITZ bonding. Previous studies have shown that pozzolanic materials and chemical admixtures can increase ITZ density by producing secondary C-S-H gel, thereby improving the structural integrity of RA with GGBS (Ahmad *et al.* 2022). **Figure 12 (d)** illustrates the M11 mix, which contains 25% GGBS and 2% I-Crete. The mixture exhibits elevated levels of C-S-H and calcium hydroxide (CH), accelerating hydration and producing more hydration products, including ettringite. This results in improved compressive strength and durability, particularly beneficial for hard pavement applications, due to reduced voids and enhanced durability.

4.2. X-ray diffraction (XRD) Analysis

X-ray diffraction (XRD) analysis was performed using X'Pert High Score and OriginPro software to determine the chemical composition of the concrete mixtures with 2θ degrees on the x-axis and intensity in arbitrary units (a.u.) on the y-axis. **Figure 13(a)** M1 exhibits a mixture with sharp peaks of quartz, ettringite, C-S-H and calcite, Portlandite all of which contribute to strength and energy development. (Majhi & Naik 2019; Krishna *et al.* 2021). Portlandite peaks confirm the presence of calcium hydroxide.

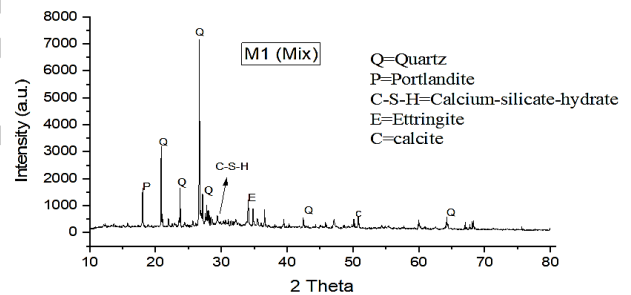


Figure 13(a) X-ray diffraction (XRD) diffractogram of the M1 concrete mix

Figure 13(b) Replacement of 100% NA with RA (M5 mix) slightly increases the ettringite and quartz intensities, while decreasing the C-S-H intensities. The M5 mix exhibits stable ettringite and quartz peaks, but portlandite intensity increases significantly due to hydrated cement in RA, resulting in higher calcium hydroxide content and voids (Wang *et al.* 2020).

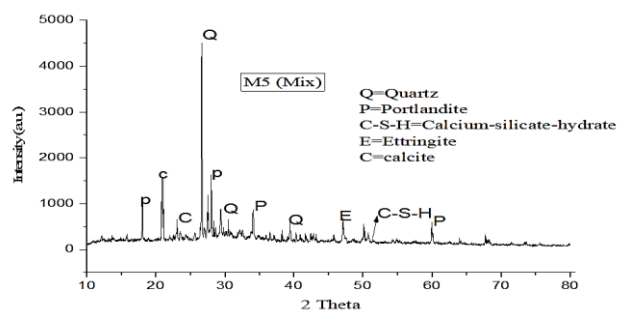


Figure 13(b) X-ray diffraction (XRD) diffractogram of the M5 concrete mix

Figure 13(c) GGBS, which contains more silica than OPC, has been shown to increase quartz and calcium

carbonate, increasing the durability of M7. GGBS reduces the creation of C-S-H and ettringite, but its pozzolanic reaction weakens portlandite peaks by consuming calcium hydroxide. **Figure 13(d)** M11 shows that the mix contains more silica, quartz and ettringite, C-S-H gel, calcite which increases strength. However, increasing RA content increases calcium hydroxide levels, leading to higher porosity at the RA-mortar interface.

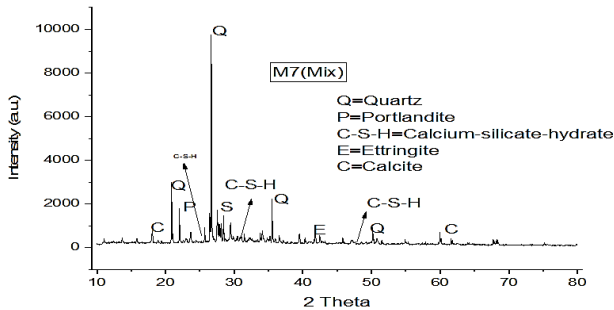


Figure 13(c) X-ray diffraction (XRD) diffractogram of the M7 concrete mix

Addition of GGBS and I-Crete to RA reduces the formation of ettringite and C-S-H, further reducing strength. However, the pozzolanic reaction of GGBS with amorphous silica consumes calcium hydroxide, improving durability. Increased crystalline silica and calcium carbonate formation further enhances the filling effect, increasing the durability of RA with GGBS and I-Crete.

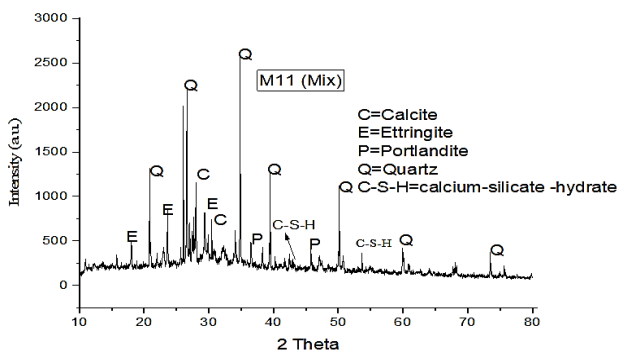


Figure 13(d) X-ray diffraction (XRD) diffractogram of the M11 concrete mix

5. Conclusion

The findings of this study have important practical implications for large-scale pavement applications, especially in terms of sustainability and durability. The use of RA in combination with additives like GGBS and I-Crete can reduce material costs, conserve natural resources, and improve the performance of concrete in pavements. The study demonstrates that with proper mix design and the incorporation of durability-enhancing additives, high RA content in PQC can lead to durable, cost-effective, and environmentally friendly pavements, making it a viable option for large-scale infrastructure projects. The findings of this research are

1. The PQC of M40 mix had a compressive strength of 51.20 MPa and 52.81 MPa at 28 and 90 days for M1 mix. The replacement of 100% NA with RA in the M5 mix

reduced the compressive strength by 5.66% and 5.60% at 28 and 90 days, respectively, due to higher voids and weaker ITZ from the adhered mortar. When 10% of cement in M5 was replaced with GGBS in M7 mix, the compressive strength decreased by 4.68% and 4.75% compared to M1, but improved over M5 mix. This improvement is due to the fine particles of GGBS filling the voids and creating a dense structure. Replacing cement with 25% GGBS and adding 2% I-Crete to the M11 mix slightly increased the compressive strength by 0.19% and 0.185% compared to M1, demonstrating that I-Crete provides a sustainable alternative without compromising strength.

2. M1 mixture exhibited drying shrinkage strains of 9.63×10^{-5} (%) and 15.40×10^{-5} (%) at 28 and 90 days. The M5 mix had 4.92 times greater strains at 28 days and 3.71 times greater strains at 90 days – due to increased porosity and weaker ITZ from RA. M7 mix showed 3.64 and 2.60 times more reduced strains than M1 at 28 and 90 days, indicating better performance. M11 mix with I-crete showed even better stability with 1.89 and 1.31 times higher strains respectively, than M1, reflecting improved performance while maintaining strength.

3. The RCPT charge is 385.55 and 375.2 coulombs for M1 at 28 and 90 days, accordingly. In the M5 mix, due to the higher void content, the charge increased by 97.37% and 89.21% compared to M1. M7 showed an improvement of the mix, the charge increased by 60.95% and 59.89% compared to M1, to the filling of GGBS vacancies and the formation of C-S-H gel. M11 mixture showed a slight decrease in charge passage of 0.37% and 1.37% compared to M1, attributed to the improved bonding and secondary reactions of I-Crete, highlighting the role of admixtures in improving concrete durability.

4. M1 mix has better water absorption (Sorptivity) resistance at 28 days. However, replacement of NA with RA in the M5 mixture resulted in higher absorption due to increased voids. M7 mix, with 10% GGBS, showed better resistance compared to M5, but less than M1 because GGBS reduces voids. Supplementation with 25% GGBS and addition of 2% I-Crete in M11 led to even lower absorption overtaking M1. This improvement is due to I-Crete improving bond strength, demonstrating an inverse Relationship among water absorption and compressive strength.

5. The depth of water penetration for M1 was 11 mm and 10.33 mm at 28 and 90 days. The penetration depth increased with 100% RA in M5 mixture, reaching 30 mm and 27.80 mm at 28 and 90 days, respectively. It is 2.72 and 2.69 times higher than M1. Adding GGBS to RA reduced the penetration by 2.21 and 2.19 times, while adding I-Crete with 25% GGBS in M11 reduced it by 1.03 and 1.02 times compared to M1. These compounds improve durability, making the mixture suitable for sustainable pavement construction.

6. SEM analysis shows that GGBS and I-Crete significantly improve the ITZ of RAC by improving particle packing, reducing voids and increasing C-S-H content. This leads to

higher compressive strength and durability, especially for hard pavement applications, compared to mixes with weak ITZ due to stuck mortar and incomplete hydration.

7. XRD analysis concludes that incorporating GGBS into RAC significantly enhances durability by consuming excess calcium hydroxide and refining the microstructure. However, increased RCA content reduces concrete strength due to increased porosity at the RCA-mortar interface. The M11 mix, with higher GGBS content, exhibits superior strength and durability, making it an ideal choice for sustainable construction.

Substituting Natural Aggregates (NA) with Recycled Aggregates (RA) has significant environmental benefits, primarily in reducing the demand for virgin resources and minimizing the environmental impact of quarrying. The use of RA in pavement concrete not only helps in recycling construction and demolition waste but also reduces the carbon footprint associated with extracting and processing NA. The study suggests that higher RA content in PQC mixes could contribute to sustainable pavement construction by reducing landfill waste, conserving natural resources, and lowering greenhouse gas emissions.

Future recommendations

Future studies should explore the long-term performance of RAC with different GGBS and I-Crete ratios, focusing on freeze-thaw resistance, fatigue behavior, and life-cycle cost analysis to further validate their use in sustainable pavement construction.

Acknowledgement

The authors thank Sri Vishnu Sai Saravana Enterprises, Visakhapatnam, for supplying GGBS, Navodya Private Limited, Chennai, for providing I-Crete, and the C&D Waste Plant, Hyderabad, for delivering recycled aggregate. We also thank Andhra University, Visakhapatnam, for providing laboratory facilities.

Reference

Ahmad J., Kontoleon K.J., Majdi A., Naqash M.T., Deifalla A.F., Ben Kahla N. and Qaidi S.M. (2022). A comprehensive review on the ground granulated blast furnace slag (GGBS) in concrete production. *Sustainability*, **14**(14), 8783.

Bonifazi G., Capobianco G., Serranti S., Eggimann M., Wagner E., Di Maio F. and Lotfi S. (2015). The ITZ in concrete with natural and recycled aggregates: Study of microstructures based on image and SEM analysis. *Proc. 15th Euroseminar Microsc. Appl. to Build. Mater*, 299–308.

Designation: C 1585–04 Standard Test Method for Measurement of Rate of Absorption of Water by Hydraulic Cement Concretes¹.

Designation: C1202–12 Standard Test Method for Electrical Indication of Concrete's Ability to Resist Chloride Ion Penetration¹.

Designation: C192/C192M–18 C192/C192M–19 Standard Practice for Making and Curing Concrete Test Specimens in the Laboratory¹.

Designation: C1723–10 Standard Guide for Examination of Hardened Concrete Using Scanning Electron Microscopy¹.

Duan Z.H. and Poon C.S. (2014). Properties of recycled aggregate concrete made with recycled aggregates with different amounts of old adhered mortars. *Materials & Design*, **58**, 19–29.

Hwang J.P., Shim H.B., Lim S. and Ann K.Y. (2013). Enhancing the durability properties of concrete containing recycled aggregate by the use of pozzolanic materials. *KSCE Journal of Civil Engineering*, **17**, 155–163. <https://www.ecomaterials.in/products-i-crete.php>

IRC:44–2017: Guidelines for Cement Concrete mix Design for pavements.

IRC:121–2017: Guidelines for use of Construction and Demolition Waste in road sector.

IS516(Part2/sec1): 2018 determination of depth of penetration of water under pressure.

IS516(Part6):2020 Determination of drying shrinkage of concrete and moisture movement of concrete samples

IS2645:2005 Indian Standard integral waterproofing compounds for cement mortar and concrete—specification

IS 1199: Part 2: 2018: Fresh Concrete—Methods of Sampling, Testing and Analysis Part 2 Determination of Consistency of Fresh Concrete (First Revision)

IS 2514: Specification for concrete vibrating tables.

IS 12089: Specification for granulated slag for the manufacture of Portland slag cement

IS. 456: 2000 Indian Standard Plain and Reinforced Concrete - Code of practice.

IRC:15-2017 Code of practice for construction of jointed plain concrete pavements.

IS 10262: 2019: Concrete Mix Proportioning — Guidelines

IS383:2016 Coarse and fine aggregate for concrete-Specification.

IS 516: Part 1: Sec 1: 2021: Hardened concrete methods of test part 1 testing of strength of hardened concrete section 1 compressive, flexural and split tensile strength.

Jain J., Verian K.P., Olek J. and Whiting N. (2012). Durability of pavement concretes made with recycled concrete aggregates. *Transportation research record*, **2290**(1), 44–51.

Jindal A., Ransinchung R.N., G.D. and Kumar P. (2017). Study of pavement quality concrete mix incorporating beneficiated recycled concrete aggregates. *Road Materials and Pavement Design*, **18**(5), 1159–1189.

Jindal A. (2016). Durability studies of PQC mix incorporating recycled concrete aggregate and mineral admixtures.

Kanellopoulos A., Nicolaidis D. and Petrou M.F. (2014). Mechanical and durability properties of concretes containing recycled lime powder and recycled aggregates. *Construction and Building Materials*, **53**, 253–259.

Kou S.C., Poon C.S. and Agrela F. (2011). Comparisons of natural and recycled aggregate concretes prepared with the addition of different mineral admixtures. *Cement and Concrete Composites*, **33**(8), 788–795.

Krishna N.R., Rao A.S. and Sasidhar C. (2021). Experimental Investigations On Mechanical And Durability Properties Of Blended Concrete. In *IOP Conference Series: Materials Science and Engineering* **1130**(1), 012036). IOP Publishing.

Kumar A. and Singh G.J. (2023). Improving the physical and mechanical properties of recycled concrete aggregate: A state-of-the-art review. *Engineering Research Express*, **5**(1), 012007.

- Kumar G. and Mishra S.S. (2022). Effect of recycled concrete aggregate on mechanical, physical and durability properties of GGBS-fly ash-based geopolymer concrete. *Innovative Infrastructure Solutions*, **7**(4), 237.
- Lim Y.Y. and Pham T.M. (2021). Effective utilisation of ultrafine slag to improve mechanical and durability properties of recycled aggregates geopolymer concrete. *Cleaner Engineering and Technology*, **5**, 100330.
- Majhi R.K. and Nayak A.N. (2019). Bond, durability and microstructural characteristics of ground granulated blast furnace slag based recycled aggregate concrete. *Construction and Building Materials*, **212**, 578–595.
- Mao Y., Liu J. and Shi C. (2021). Autogenous shrinkage and drying shrinkage of recycled aggregate concrete: A review. *Journal of Cleaner Production*, **295**, 126435.
- Ministry of Road Transport and Highways (MORTH) Standards.
- Nandanam K., Biswal U.S. and Dinakar P. (2021). Effect of fly ash, GGBS, and metakaolin on mechanical and durability properties of self-compacting concrete made with 100% coarse recycled aggregate. *Journal of Hazardous, Toxic, and Radioactive Waste*, **25**(2), 04021002.
- Olorunsogo F.T. and Padayachee N. (2002). Performance of recycled aggregate concrete monitored by durability indexes. *Cement and concrete research*, **32**(2), 179–185.
- Sarma V.V.S., Subhan Alisha S., Vijay K., Gireesh Kumar P. and Sai Kumar K.S. (2024). Mechanical performance enhancement of recycled aggregate concrete using GGBS and fly ash for sustainable construction. *Multiscale and Multidisciplinary Modeling, Experiments and Design*, **7**(3), 1693–1700.
- Sharma P., Verma M. and Sharma N. (2021). Examine the mechanical properties of recycled coarse aggregate with MK GGBS. In *IOP conference series: materials science and engineering* (1116(1), 012152). IOP Publishing.
- Silva R.V., De Brito J. and Dhir R.K. (2019). Use of recycled aggregates arising from construction and demolition waste in new construction applications. *Journal of Cleaner Production*, **236**, 117629.
- Singh Y. and Singh H. (2021). Recycling Construction and Demolition Waste: Potential Applications and the Indian Scenario. In *Integrated Approaches Towards Solid Waste Management* (273–281). Cham: Springer International Publishing.
- Tam V.W., Soomro M. and Evangelista A.C.J. (2018). A review of recycled aggregate in concrete applications (2000–2017). *Construction and Building materials*, **172**, 272–292.
- Teng S., Lim T.Y.D. and Divsholi B.S. (2013). Durability and mechanical properties of high strength concrete incorporating ultra fine ground granulated blast-furnace slag. *Construction and Building Materials*, **40**, 875–881.
- Thomas C., Setián J., Polanco J., Alaejos P. and De Juan M.S. (2013). Durability of recycled aggregate concrete. *Construction and building materials*, **40**, 1054–1065.
- Wang B., Yan L., Fu Q. and Kasal B. (2021). A comprehensive review on recycled aggregate and recycled aggregate concrete. *Resources, Conservation and Recycling*, **171**, 105565
- Wang J., Xie J., Wang C., Zhao J., Liu F. and Fang C. (2020). Study on the optimum initial curing condition for fly ash and GGBS based geopolymer recycled aggregate concrete. *Construction and Building Materials*, **247**, 118540.
- Yeau K.Y. and Kim E.K. (2005). An experimental study on corrosion resistance of concrete with ground granulates blast-furnace slag. *Cement and Concrete Research*, **35**(7), 1391–1399.
- Yu Y., Wang P., Yu Z., Yue G., Wang L., Guo Y. and Li Q. (2021). Study on the effect of recycled coarse aggregate on the shrinkage performance of green recycled concrete. *Sustainability*, **13**(23), 13200.
- Zega C.J., Di Maio Á.A. and Zerbino R.L. (2014). Influence of natural coarse aggregate type on the transport properties of recycled concrete. *Journal of materials in civil engineering*, **26**(6), 04014006.
- Zhang P., Sun X., Wang F. and Wang J. (2023). Mechanical properties and durability of geopolymer recycled aggregate concrete: A review. *Polymers*, **15**(3), 615.
- Zhang W., Hama Y. and Na S.H. (2015). Drying shrinkage and microstructure characteristics of mortar incorporating ground granulated blast furnace slag and shrinkage reducing admixture. *Construction and building materials*, **93**, 267–277.
- Zhang W., Zakaria M. and Hama Y. (2013). Influence of aggregate materials characteristics on the drying shrinkage properties of mortar and concrete. *Construction and building materials*, **49**, 500–510.

Response to Reviewer and Editor Comments:

REVIEWER (I)	Authors	Amended text
Why 2% of I-crete was chosen is not mentioned. can place error bars on all the test results represented in graphs.	The reason for choosing 2% I-crete is mentioned. The error bars are placed on all the applicable graphs.	The reason for 2% I-Crete was added in section 2.1 under data collection in the last paragraph and highlighted in green color. Additionally, error bars have been implemented in Figures 7, 8, 9, and 11 .
Can improve the writing language and can improve the graph's quality and presentation.	The writing language and the quality of the graphs were enhanced for better presentation	The writing language The quality of the graphs in Figures 1 to 12 has been improved to the best possible standard. highlighted in green color
REVIEWER (D)		
Are the references correctly written? its not in as per guideline	References have been revised to comply with the specified guidelines.	References have been revised
Does the Graphical Abstract correspond the central idea of the paper? not matched	The Graphical Abstract has been revised to align with the central idea of the paper	The graphical abstract has been revised and pasted in the revised manuscript.
1. Provide a clearer rationale for selecting the specific RA	Recycled aggregate (RA) replacement percentages range from 25% to 100% to	The rationale for selecting the specific RA replacement percentages and their potential

replacement percentages and their potential impact on performance.	assess concrete performance. At lower RA levels, the impact is minimal, while higher levels significantly affect concrete behavior	impact on performance has been discussed in the last paragraph of section 3.1 under compressive strength and highlighted in blue color.
2. Elaborate on the significance of I-Crete addition for durability enhancement compared to traditional additives.	Compared to the traditional additives, I-Crete, with its lower dosage, enhanced the durability behavior.	The reasons have been added and discussed in the last paragraph of section 2.3 and highlighted in blue color.
3. Include more statistical analysis to support the compressive strength results across different mixes.	Statistical analysis, such as standard deviation, is performed on each mix, and it is presented as error bars on the respective graphs.	Statistical analysis, such as standard deviation, was performed on each mix and presented as error bars on the respective graphs. This is discussed below Figure 7 and highlighted in blue color.
4. Provide additional explanation for how drying shrinkage is impacted by higher RA levels.	Parameters such as higher water demand, higher porosity, and weaker Interfacial Transition Zone affect drying shrinkage at higher RA levels.	Additional explanation on how drying shrinkage is impacted by higher RA levels has been added in section 3.2 and highlighted in blue color.
5. Check for grammatical errors throughout the manuscript to improve readability.	Yes, the grammatical errors were rectified.	Yes, the grammatical errors have been rectified and highlighted in blue color.
6. Ensure all formatting adheres to the journal's guidelines, particularly in the tables and figures.	The article is properly aligned with the journal guidelines.	Yes, all possible formatting has been adjusted to adhere to the journal's guidelines, particularly in the tables and figures, and highlighted in blue color.
7. Clarify the methodology used for measuring water penetration and RCPT values in all tested samples.	The water penetration depth was measured according to IS:516:part2:sec1:2018 while the RCPT was conducted following ASTM C1202, with the total charge passed through 50-mm thick discs subjected to a 60 V DC current for 6 hours to assess chloride ion penetration.	The water penetration depth was measured as per IS:516: Part 2: Sec 1:2018, and the RCPT was conducted following ASTM C1202. This is added in section 3.3 and highlighted in blue color in the first paragraph.
8. Verify the accuracy of all units presented in tables, especially in the compressive strength and shrinkage data.	The accuracy of all the units is rectified, and necessary changes are incorporated.	The accuracy of all the units is rectified.
9. Include a discussion on the environmental impact of substituting NA with RA in pavement concrete.	Discussion is added.	A discussion on the environmental impact of substituting natural aggregates (NA) with recycled aggregates (RA) in pavement concrete has been added after the conclusion and highlighted in blue color.
10. Specify the testing standards followed for each durability parameter, such as sorptivity and RCPT.	The codes of conduct for sorptivity and RCPT were ASTM-C-1202 and ASTM-C-1585-04.	The testing standards followed for each durability parameter, such as sorptivity and RCPT, have been specified in section 2.2 under data measurement and highlighted in blue color.
11. Improve the clarity of technical terms, ensuring all abbreviations are defined on first use.	The suggestions are considered, and all the abbreviations are mentioned in their first use.	All technical terms and abbreviations have been clarified, with definitions provided on first use in the abstract, in Table 1 , and at the beginning of paragraphs for new technical terms.
12. Provide a comparison of the drying shrinkage behavior of each mix with other studies in similar domains.	The revised manuscript now includes a comparative analysis of drying shrinkage behavior across mixes, highlighting reduced shrinkage with recycled aggregates, GGBS, and I-Crete in line with similar studies.	A comparison of the drying shrinkage behavior of each mix with other studies in similar domains has been discussed in section 3.2 below Figure 8 and highlighted in blue color.
13. Elaborate on how GGBS and I-Crete combine to counteract the reduction in compressive strength with higher RA content.	The elaboration of how GGBS and I-Crete counteract the reduction in compressive strength is mentioned in the manuscript.	An explanation of how GGBS and I-Crete work together to counteract the reduction in compressive strength with higher RA content has been added above Figure 8 and highlighted in blue color.
14. Highlight the practical implications of this research for	Yes, the practical implications of applications are added in the manuscript.	The practical implications of this research for large-scale pavement applications have been

large-scale pavement applications.		discussed and added to the beginning of the conclusion, highlighted in blue color.
15. Conduct a spell check as some terms have minor spelling errors, affecting the manuscript's professionalism.	The spell check is done.	A spell check has been completed in the revised manuscript.
ASSOCIATE EDITOR (A)		
Barely the environmental implications of the replacement must be better discussed	the revised manuscript now includes an expanded discussion on the environmental implications of material replacements, highlighting their benefits for sustainability and carbon footprint reduction	The environmental implications of the replacement have been discussed below the conclusion and highlighted in blue color.
Graphical Abstract, novelty of the paper, Are figures and tables, Methods, paper's contribution significant	the revised manuscript now incorporates all suggested improvements, including an updated Graphical Abstract, a clear statement of the paper's novelty, enhanced figures and tables, refined methods, and a more detailed explanation of the paper's contribution, ensuring alignment with the reviewer's recommendations.	As per the reviewer's suggestion, the graphical abstract, novelty of the paper, significance of figures and tables, methods, and the paper's contribution have been discussed in the revised manuscript.

UNCORRECTED PROOF